Implementation of 12 Transition Controls for Rotary Double Inverted Pendulum Using Direct Collocation

Doyoon Ju[a], Taegun Lee[b] and Young Sam Lee[c]
Department of Electrical and Computer Engineering, Inha University, Incheon, Korea
{*seiko.kr, dlxorjs815*}*@gmail.com, lys@inha.ac.kr*

Keywords: Rotary Double Inverted Pendulum, Transition Control, Direct Collocation, Optimal Control.

Abstract: The rotary double inverted pendulum system has one stable and three unstable equilibrium points due to its kinematic properties. This paper extends the traditional swing-up control problem by defining a novel transition control problem among these points. We formulate the system's dynamic equations and boundary conditions for different equilibrium points to minimize energy consumption during transitions, resulting in a two-point boundary value optimal control problem. This problem is solved offline to calculate the feedforward trajectory for feedforward control. To convert the continuous optimal control problem with constraints into a nonlinear optimization problem, we employ the direct collocation method. A time-varying Linear Quadratic controller is used as the feedback controller to accurately track the generated feedforward path during real-time control, compensating for uncertainties. Previous studies on rotary double inverted pendulums have focused on the swing-up problem, with no research addressing transition control between the four equilibrium points. This paper defines the transition control problem for the rotary double inverted pendulum and proposes a control strategy. The method's effectiveness and practicality were validated through the design and implementation of 12 transition trajectories in experimental settings, successfully demonstrating its feasibility and utility.

1 INTRODUCTION

The inverted pendulum system, with its unstable dynamic characteristics, incorporates both nonlinear and non-minimum phase properties, making it a widely used educational tool for teaching control theory. Additionally, it serves as a popular testbed for researchers to validate new control techniques. Major studies on the inverted pendulum system include swing-up control, which transitions the pendulum from an initial state where it points downward to an upright state(Åström and Furuta, 2000; Meta et al., 2014), and balance control, which aims to maintain stability in the upright state after the swing-up(Oh and Lee, 2018). Among these, swing-up control is considered a more challenging research topic compared to balance control because it requires designing a controller that accounts for the system's nonlinearity, instability, and input/output constraints.

In the case of the rotary inverted pendulum system, unlike the linear inverted pendulum where the pendulum is fixed to rotate in a single plane, the powered arm of the rotary inverted pendulum also rotates. This characteristic allows the pendulum to move within a three-dimensional space, introducing additional challenges in performing swing-up control. To address the swing-up problem of such a rotary inverted pendulum system, various methods have been applied, including self-tuning techniques(Ratiroch-Anant et al., 2004), PID controllers(Rahairi et al., 2011), and methods utilizing sliding observers(Thein and Misawa, 1995). Recently, research has also been conducted to solve this problem using artificial intelligence-based controllers(Brown and Strube, 2020; Baek et al., 2024).

However, in the case of the rotary double inverted pendulum, most studies have implemented swing-up control using only simulation environments(Liang et al., 2023; Tran et al., 2024; Singh and Swarup, 2021; Zied et al., 2020). Rarely, when physical systems were used, research was primarily limited to balance control after manually performing the swing-up(Ibrahim et al., 2019; Sondarangallage and Manukid, 2019). A common limitation in these studies is the absence of a physical rotary double inverted pendulum system capable of performing swing-up

[a] https://orcid.org/0000-0001-7011-6779
[b] https://orcid.org/0009-0007-3107-2735
[c] https://orcid.org/0000-0003-0665-1464

Ju, D., Lee, T. and Lee, Y.
Implementation of 12 Transition Controls for Rotary Double Inverted Pendulum Using Direct Collocation.
DOI: 10.5220/0012994200003822

In *Proceedings of the 21st International Conference on Informatics in Control, Automation and Robotics (ICINCO 2024) - Volume 1*, pages 92-100
ISBN: 978-989-758-717-7; ISSN: 2184-2809

control. Even if such a system exists, there is a lack of documented successful implementations of swing-up control in academic literature.

Building on the research laboratory's extensive experience in developing various inverted pendulum systems over many years, the authors aim to solve the problem by constructing a physical system themselves, instead of purchasing a commercially available rotary inverted pendulum. The most critical objective in this process is to ensure that the arm of the rotary inverted pendulum can rotate infinitely, a characteristic feature of the system. To address this, previous research successfully utilized a slip ring structure to overcome the rotational displacement constraints and perform swing-up control(Oh and Lee, 2018). Building on this experience, the authors' research laboratory seeks to directly construct a rotary double inverted pendulum and implement swing-up control using the physical system.

In the case of a single-link inverted pendulum system, there is only one type of swing-up problem. This involves moving from the stable equilibrium point where the pendulum hangs downward to the unstable equilibrium point in the upright position. However, when the pendulum has two links, there are two additional unstable equilibrium points determined by the angles of each link. These are in addition to the stable equilibrium points where both links point downward and the unstable equilibrium points where both links are upright. This introduces not only the simple swing-up problem but also a newly defined 'transition control' problem between these equilibrium points. The transitions between the four equilibrium points created by the two links result in 11 different types of transitions, excluding the traditional swing-up. This paper experimentally addresses all 12 transition controls, including swing-up control.

The transition control among the four equilibrium points of the rotary double inverted pendulum used in the experiments can be designed by referencing the swing-up control strategy of the linear inverted pendulum. In 2007, Graichen effectively addressed the swing-up control problem by introducing a two-degree-of-freedom (2-DOF) control structure that combines feedforward and feedback control, taking into account the rail length constraints of the linear double inverted pendulum(Graichen et al., 2007). The basic concept of the 2-DOF control structure used by Graichen involves using the dynamic equations of the multi-link inverted pendulum to calculate the state and control input trajectories offline that lead the pendulum to an upright position. The calculated feedforward trajectory is then applied to guide the pendulum to the upright state. During the operation of the system, the difference between the actual trajectory and the calculated feedforward trajectory is corrected through feedback control. This ensures successful swing-up by closely following the feedforward trajectory. Based on this study, the present paper uses the direct collocation method(Kelly, 2017) to numerically solve the nonlinear optimal control problem to find the feedforward trajectory for the rotary double inverted pendulum. The feedback controller design follows a similar approach to Graichen's method and employs Linear Quadratic(LQ) control, an optimal control technique for time-varying systems. Unlike Graichen's method, which assumes a specific form for the trajectory, the direct collocation method imposes no constraints on the trajectory shape, increasing the likelihood of finding a numerical solution for the trajectory.

This paper aims to implement all 12 types of transition control using the physical rotary double inverted pendulum system. In Chapter 2, we first derive the dynamic equations of the system using the Euler-Lagrange equations based on the structural characteristics of the rotary double inverted pendulum used in the experiments. Chapter 3 defines each equilibrium point and transition control problem and proposes a method to obtain the feedforward trajectory using the direct collocation method, which numerically solves the nonlinear optimal problem. In Chapter 4, we perform the 12 transition control experiments using a 2-DOF controller designed with time-varying LQ control. Finally, in Chapter 5, we analyze the results to verify the effectiveness of the proposed method.

2 MATHEMATICAL MODEL OF THE ROTARY DOUBLE INVERTED PENDULUM

The rotary double inverted pendulum used in this paper is shown in Figure 1, and Figure 2 illustrates the mechanical concept of the system.

The unit system used in this paper is the International System of Units (SI), and all variables and parameters are defined accordingly. Here, θ represents the rotational displacement from the initial position of the arm, and u denotes the angular acceleration of the arm. R_1 is the distance between the arm and the first pendulum, while r_1 and r_2 represent the x-axis directional distances from the arm to the center of mass of the first and second pendulums, respectively. M_1 and M_2 are the masses of the first and second pendulums, l_1 and l_2 are the lengths from the rotational axis to the center of mass of each pendulum, and L_1 is the length

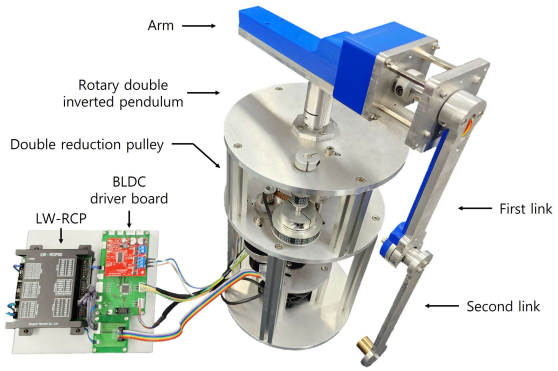

Figure 1: Rotary double inverted pendulum system constructed by the laboratory.

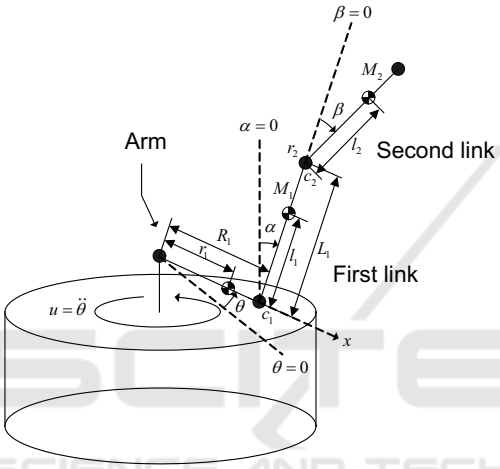

Figure 2: The conceptual diagram of a rotary double inverted pendulum.

from the rotational axis of the first pendulum to the rotational axis of the second pendulum. α is defined as the rotational displacement of the first pendulum with respect to the normal of the ground, and β is defined as the relative rotational displacement of the second pendulum with respect to the first pendulum. Additionally, c_1 and c_2 denote the friction coefficients at the rotational axes of the first and second pendulums, respectively. Figure 3 illustrates the rotations of the first and second pendulums, and expressions like I_{xx1} represent the moments of inertia of the pendulums(Oh and Lee, 2018). The dynamic model of the rotary double inverted pendulum can be derived using the Euler-Lagrange equation and is expressed as follows.

$$\begin{bmatrix} n_1 \\ n_2 \end{bmatrix} \ddot{\theta} + \begin{bmatrix} m_{11} & m_{12} \\ m_{21} & m_{22} \end{bmatrix} \begin{bmatrix} \ddot{\alpha} \\ \ddot{\beta} \end{bmatrix} + \begin{bmatrix} d_1 \\ d_2 \end{bmatrix} = 0. \quad (1)$$

Each component of Equation (1) is defined as follows.

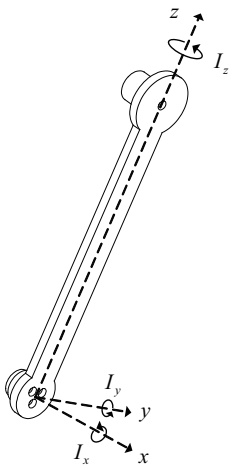

Figure 3: Rotation and inertia I of the first and second links.

$$\begin{aligned}
n_1 &= h_1\cos(\alpha) + h_2\cos(\alpha+\beta),\\
n_2 &= h_2\cos(\alpha+\beta),\\
m_{11} &= h_3 + h_6 + 2h_4\cos(\beta),\\
m_{12} &= h_6 + h_4\cos(\beta),\\
m_{21} &= h_6 + h_4\cos(\beta),\\
m_{22} &= h_6,\\
d_1 &= -h_4\sin\beta(2\dot{\alpha}\dot{\beta}+\dot{\beta}^2) - h_5\sin\alpha\\
&\quad - h_7\sin(\alpha+\beta) + c_1\dot{\alpha}\\
&\quad - \dot{\theta}^2\{\frac{1}{2}h_8\sin(2\alpha) + h_4\sin(2\alpha+\beta)\\
&\quad + \frac{1}{2}h_9\sin(2\alpha+2\beta)\},\\
d_2 &= h_4\sin\beta(\dot{\alpha}^2) - h_7\sin(\alpha+\beta) + c_2\dot{\beta}\\
&\quad - \dot{\theta}^2\{\frac{1}{2}h_9\sin(2\alpha+2\beta)\\
&\quad + \frac{1}{2}h_4(\sin(2\alpha+2\beta) - \sin\beta)\}.
\end{aligned}$$

h_1 to h_9 are defined as follows, and g represents the gravitational acceleration of 9.81 $[m/s^2]$.

$$\begin{aligned}
h_1 &= M_1 l_1 r_1 + M_2 L_1 (R_1 + r_2) - I_{xz1},\\
h_2 &= M_2 l_2 (R_1 + r_2) - I_{xz2},\\
h_3 &= I_{xx1} + M_1 l_1^2 + M_2 L_1^2,\\
h_4 &= M_2 L_1 l_2,\\
h_5 &= g(M_1 l_1 + M_2 L_1),\\
h_6 &= I_{xx2} + M_2 l_2^2,\\
h_7 &= M_2 g l_2,\\
h_8 &= M_1 l_1^2 + M_2 L_1^2 + I_{yy1} - I_{zz1},\\
h_9 &= M_2 l_2^2 + I_{yy2} - I_{zz2}.
\end{aligned}$$

Thus, Equation (1) can be rearranged as follows.

$$\begin{bmatrix} \ddot{\alpha} \\ \ddot{\beta} \end{bmatrix} = -\begin{bmatrix} m_{11} & m_{12} \\ m_{21} & m_{22} \end{bmatrix}^{-1} \left\{ \begin{bmatrix} n_1 \\ n_2 \end{bmatrix} \ddot{\theta} + \begin{bmatrix} d_1 \\ d_2 \end{bmatrix} \right\}.$$

By solving this,

$$\begin{aligned}\ddot{\alpha} &= \frac{(-m_{22}n_1+m_{12}n_2)\ddot{\theta}+(-m_{22}d_1+m_{12}d_2)}{\Phi},\\ \ddot{\beta} &= \frac{(m_{21}n_1-m_{11}n_2)\ddot{\theta}+(m_{21}d_1-m_{11}d_2)}{\Phi},\\ \Phi &= m_{11}m_{22}-m_{12}m_{21}.\end{aligned}$$

In this context, the state vector is defined as $x_1=\theta$, $x_2=\alpha$, $x_3=\beta$, $x_4=\dot{\theta}$, $x_5=\dot{\alpha}$, $x_6=\dot{\beta}$, $x_7=\int_0^t\theta(\tau)d\tau$, and the angular acceleration $\ddot{\theta}$ is represented as u. Consequently, the model equation of the double inverted pendulum can ultimately be expressed as the following nonlinear state equation. The last element of the state variable, $\int_0^t\theta(\tau)d\tau$, is an additional term introduced to eliminate the steady-state error in the position of the arm.

$$\underbrace{\begin{bmatrix}\dot{x}_1\\ \dot{x}_2\\ \dot{x}_3\\ \dot{x}_4\\ \dot{x}_5\\ \dot{x}_6\\ \dot{x}_7\end{bmatrix}}_{\dot{x}} = \underbrace{\begin{bmatrix}x_4\\ x_5\\ x_6\\ u\\ \frac{(-m_{22}n_1+m_{12}n_2)\ddot{\theta}+(-m_{22}d_1+m_{12}d_2)}{\Phi}\\ \frac{(m_{21}n_1-m_{11}n_2)\ddot{\theta}+(m_{21}d_1-m_{11}d_2)}{\Phi}\\ x_1\end{bmatrix}}_{f(x,u)}. \tag{2}$$

The dynamic model derived in this manner is subsequently used as the feedforward trajectory generation model when applying the direct collocation method.

3 DESIGN AND IMPLEMENTATION OF TRANSITION CONTROL

3.1 Transition Control Design

The four possible equilibrium points of the rotary double inverted pendulum, determined by the states of the first and second pendulums, are depicted in Figure 4. In this paper, the numbering of equilibrium points is represented using a binary notation, where the states Up and Down are designated as 1 and 0, respectively. If the numbering is assigned starting from the first pendulum, the equilibrium point where both the first and second pendulums are in the Down-Down state corresponds to the binary number 00 and is denoted as EP0. Similarly, the equilibrium point corresponding to the Up-Down state is represented by the binary number 10 and is denoted as EP2. In this paper, the equilibrium points of the inverted pendulum will be denoted as EP0 (Down-Down), EP1 (Down-Up), EP2 (Up-Down), and EP3 (Up-Up) according to this method.

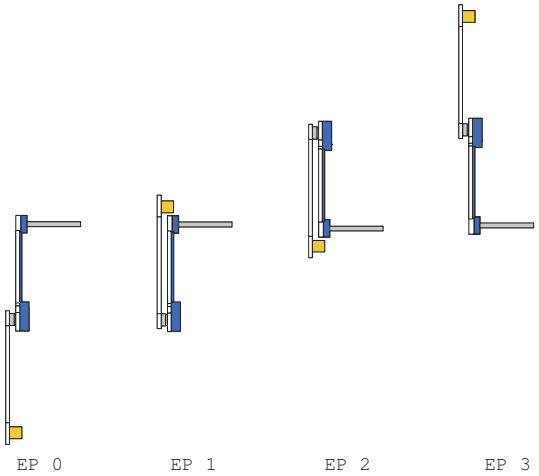

Figure 4: Four equilibrium points of a rotary double inverted pendulum.

The implemented transition control follows three steps:

1. Linear control at the current equilibrium point.
2. Transition control from the current equilibrium point to the next equilibrium point.
3. Linear control at the next equilibrium point.

Each transition process is structurally similar to the swing-up problem, which involves moving the pendulum from its initial state (EP0) to the upright state (EP3). First, linear control is performed to ensure the stability of the current state before transitioning between the four equilibrium points. Next, transition control is executed to move from the current equilibrium point to the next equilibrium point. Upon reaching the new equilibrium point, additional linear control is required to maintain stability at that point. Thus, each transition process must satisfy both major elements: linear control at the equilibrium points and transition control between the equilibrium points. Since there are a total of 12 different transition trajectories for the double inverted pendulum, experiments must be designed and conducted for each trajectory to meet the required conditions.

The 12 transition trajectories presented in this paper are configured according to the sequence diagram in Figure 5.

3.2 Implementation of Transition Control

To calculate the optimal state x^* and control input u^* required for generating transition control trajectories,

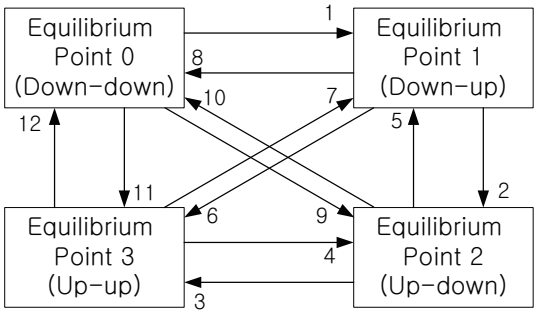

Figure 5: 12-step transition diagram for the double inverted pendulum.

it is essential to accurately estimate the parameters of the system depicted in Figures 2 and 3. Parameters such as M_1, M_2, I_{xx1}, I_{xx2}, l_1, l_2, c_1, and c_2 can be estimated using the parameter estimation techniques for the linear double inverted pendulum(Ju et al., 2022). The estimation of the inertia tensor can be performed by referring to the research conducted by Oh(Oh and Lee, 2018). The parameters of the rotary double inverted pendulum obtained through these estimation processes are summarized in Table 1.

Table 1: Model parameters of the rotary double inverted pendulum used in the experiments.

Parameter	Value
M_1	0.187 [kg]
M_2	0.132 [kg]
I_{xx1}	1.0415e-03 [kgm^2]
I_{xx2}	8.8210e-04 [kgm^2]
I_{yy1}	4.3569e-03 [kgm^2]
I_{yy2}	4.9793e-03 [kgm^2]
I_{zz1}	3.3179e-03 [kgm^2]
I_{zz2}	4.8178e-03 [kgm^2]
I_{xz1}	3.7770e-04 [kgm^2]
I_{xz2}	1.9823e-04 [kgm^2]
l_1	0.072 [m]
l_2	0.133 [m]
c_1	2.4100e-06
c_2	1.0900e-06
L_1	0.1645 [m]

The transition control between the equilibrium points of the pendulum is performed using a 2-DOF control technique that combines nonlinear feedforward control and feedback control as proposed in (Graichen et al., 2007). Figure 6 illustrates the 2-DOF control structure. In the control process, the precomputed ideal angular acceleration trajectory $u^*(t)$ is combined with the correction input $\Delta u(t)$, which is calculated based on the error $\Delta x(t) = x^*(t) - x(t)$ between the predicted state variables of the inverted pendulum system and the actual output values. This generates the actual angular acceleration input $u(t) = u^*(t) + \Delta u(t)$. In this paper, the feedforward trajectory is generated by considering the dynamic constraints and setting up a nonlinear optimal control problem that numerically minimizes the desired cost function while satisfying various constraints. The direct collocation method is used to numerically solve this problem(Kelly, 2017). This method effectively estimates the control inputs and state variable paths of continuous dynamic systems and is a proven technique for obtaining the optimal trajectory to achieve control objectives.

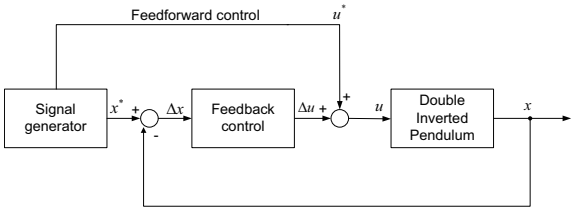

Figure 6: 2-DOF control framework for the double inverted pendulum.

The direct collocation method is an iterative numerical solution implemented using a nonlinear optimization solver. This method is characterized by the influence of the initial trajectory provided by the designer on the solution time of the numerical method and the resulting trajectory's shape. By considering these characteristics and selecting an appropriate initial trajectory, the designer can effectively apply the direct collocation method to derive a suitable trajectory for specific transition control problems. In this paper, the initial trajectory is designed using the simplest form of a straight-line trajectory connecting the start and end boundary conditions. Additionally, a cost function is designed to satisfy all set constraints and boundary conditions, forming a general nonlinear optimal control problem. Equation (3) below represents the optimal control problem set to calculate the optimal trajectory.

$$\begin{array}{cc} \overset{\text{Minimize}}{u(t)} & J(x(t),u(t)) \\ \text{subject to} & \begin{array}{c}\text{input/output constraint,}\\ \text{dynamic equations,}\\ \text{boundary conditions.}\end{array} \end{array} \tag{3}$$

In the above equation, $J(x(t),u(t))$ represents the cost function and is defined as an optimal control problem that satisfies the constraints set using the model parameters of the actual system as listed in Table 1. The cost function can be used either to minimize time or to optimize the cost over a given period. The constraints and limitations applied to this cost

function include the dynamic equations of the rotary double inverted pendulum (2) and the limits specified by equation (4), which restrict the maximum distance the arm can move during the control process, as well as the maximum angular velocity and input angular acceleration of the arm within the operational range of the actuator. These conditions play a crucial role in ensuring the practical operability and stability of the control system.

$$|x_1^*| \leq \theta_{limit}, \quad |x_4{}^*| \leq \dot{\theta}_{limit}, \quad |u^*| \leq u_{limit}. \tag{4}$$

The set limit values are all defined as positive, with $\theta_{limit} > 0$, $\dot{\theta}limit > 0$, and $ulimit > 0$ specifying the maximum allowable values for the arm's output displacement, output angular velocity, and input angular acceleration, respectively. These limit values reflect the actual operational constraints of the rotary double inverted pendulum used in the experiments, and these constraints are explicitly stated in equation (5).

$$\begin{aligned} \theta_{limit} &= 1.5[\text{rad}], \\ \dot{\theta}_{limit} &= 7.0[\text{rad/s}], \\ u_{limit} &= 50[\text{rad/s}^2]. \end{aligned} \tag{5}$$

To satisfy various constraints during the 12 different transition control processes, additional constraints can be applied to the pendulum's rotation angles α and β as well as their angular velocities $\dot{\alpha}$ and $\dot{\beta}$. Furthermore, at the start ($t = 0$) and end ($t = T$) of the transition control, the boundary conditions corresponding to the specific equilibrium points for the transition must be satisfied. For example, if the current equilibrium point is EP0 and the target equilibrium point for the transition is EP3, this situation can be expressed as shown in equation (6).

$$\begin{aligned} x^*(0) &= \left[\ 0, -\pi, 0, 0, 0, 0\ \right]^T, \\ x^*(T) &= \left[\ 0, 0, 0, 0, 0, 0\ \right]^T, \\ u^*(0) &= 0, u^*(T) = 0. \end{aligned} \tag{6}$$

By utilizing the direct collocation method, the transition trajectories implemented can be optimized to satisfy the set constraints and boundary conditions during the transition process, as illustrated in Figure 7.

4 EXPERIMENTAL VALIDATION AND RESULTS

The design of the feedback controller for trajectory tracking is similar to the method proposed by Graichen(Graichen et al., 2007), mentioned in the introduction. However, a key difference in this study is the application of the optimal control technique,

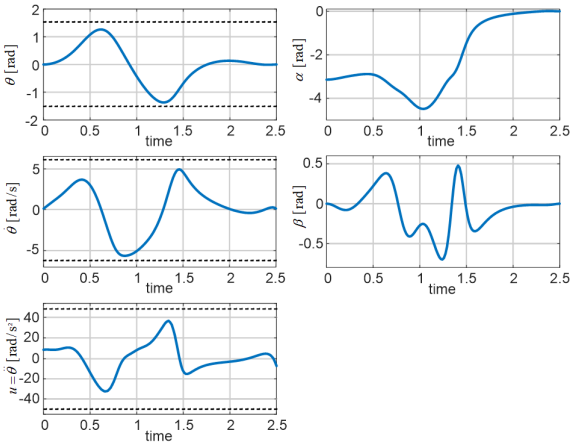

Figure 7: Feedforward transition trajectory from EP0 to EP3.

linear-quadratic (LQ) control, for time-varying systems throughout the entire process. In Graichen's study, it was determined that high compensation values in intervals where the gain coefficient increases rapidly could lead to a loss of controllability, prompting the decision to suspend feedback in certain intervals. In contrast, this study maintains a consistent control strategy by utilizing the calculated time-varying LQ control gain values across all intervals during the implementation of transition control. The design of this time-varying LQ controller is based on the linearized dynamic system centered around the swing-up trajectory of the double inverted pendulum system. The state equations used in this process, which vary with time, used in this process are modeled in a form where the values of A and B are time-varying, as shown in equation (7).

$$A(t) = \left.\frac{\partial f}{\partial x}\right|_{x^*(t),u^*(t)}, \qquad B(t) = \left.\frac{\partial f}{\partial u}\right|_{x^*(t),u^*(t)}. \tag{7}$$

In this context, $x^*(t)$ and $u^*(t)$ represent the feedforward trajectories for the state and input obtained using the direct collocation method. The difference between the obtained feedforward trajectory and the actual state variable values is calculated as $\Delta x(t) = x^*(t) - x(t)$, and the correction input $\Delta u(t)$ generated to compensate for this error is defined by equation (8).

$$\Delta u(t) = -K(t)\Delta x(t). \tag{8}$$

In this case, the time-varying state equation can be expressed as equation (9).

$$\Delta \dot{x}(t) = A(t)\Delta x(t) + B(t)\Delta u(t). \tag{9}$$

The cost function used is given by equation (10).

$$J = \Delta x^T(T) H_{Tr} \Delta x(T) + \int_0^T \Delta x(t)^T Q_{Tr} \Delta x(t) + \Delta u(t)^T R_{Tr} \Delta u(t)\, dt. \quad (10)$$

Here, the subscript Tr is used to indicate the design variables of the transition process. In equation (10), the variables with this subscript must satisfy $H_{Tr} \geq 0$, $Q_{Tr} \geq 0$, and $R_{Tr} > 0$. The matrix H_{Tr} represents the weight on the terminal state, the matrix Q_{Tr} represents the weight on the system state, and the matrix R_{Tr} represents the weight on the control input. These weights are set to the values of equation (11) through an experimental process.

$$\begin{aligned} Q_{Tr} &= \mathrm{diag}(1, 300, 500, 1, 1, 1, 1), \\ R_{Tr} &= 1. \end{aligned} \quad (11)$$

Additionally, to calculate the time-varying gain $K(t)$, the differential Riccati equation presented in equation (12) must be solved.

$$\begin{aligned} \dot{P}(t) &= -A(t)^T P(t) - P(t)A(t) \\ &\quad + PB(t)R_{Tr}^{-1} B^T(t) P(t) - Q_{Tr}, \\ P(T) &= H_{Tr}. \end{aligned} \quad (12)$$

Ultimately, the time-varying gain $K(t)$ can be calculated using equation (13). The LQ control gain $K(t)$ applied in the earlier Figure 7 can be seen in Figure 8.

$$K(t) = R_{Tr}^{-1} B^T(t) P(t). \quad (13)$$

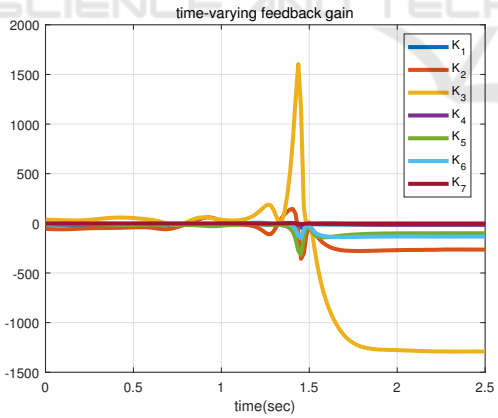

Figure 8: Time-varying LQ gain of feedforward transition trajectory from EP0 to EP3.

To conduct the experiments, the swing-up trajectory obtained using the direct collocation method presented in Chapter 3 is combined with the LQ control-based feedback controller to implement the 12 different transition controls. The trajectory paths are configured according to the flowchart in Figure 5, and the transition paths between each equilibrium point are designed to move only once. The duration of one cycle of state transition and linear control at the equilibrium point is set to 5 seconds, with the time taken for state transitions varying from a minimum of 1.8 seconds to a maximum of 3 seconds, as shown in Table 2. After each transition, linear control is performed at the corresponding equilibrium point until the next transition control begins, to stabilize the system. Figure 9 shows a captured image of a YouTube video that presents the experimental results of 12 transition controls. The actual YouTube video can be accessed at https://youtu.be/J8vRJtQ-t3I (Video title: 12 transition controls of a rotary double inverted pendulum (with double reduction timing pulleys), Channel name: Embedded Control Lab.), where the experimental results can be viewed in detail.

The first state transition begins at the 5-second point, and Figure 10 shows the continuous results of all transition controls. Each line represents the simulation model trajectory depicted by solid lines and the actual experimental trajectory shown by dashed lines. Due to the compensation effect of the closed-loop control, the arm's rotation angle θ and angular velocity $\dot{\theta}$ exhibit significant differences immediately after the state transition, but the result graphs for α and β, which are the most critical variables in transition control, demonstrate that the predicted paths are followed with high accuracy. Following this, linear control at the equilibrium point gradually adjusts the θ value to approach zero, helping to limit the random movement of the double pendulum and enabling all 12 transition controls to be successfully executed.

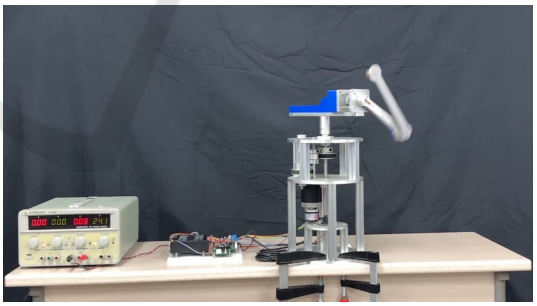

Figure 9: The Youtube video for 12 transition controls of the RDIP.

5 CONCLUSION AND FUTURE WORK

In this paper, we established an experimental environment using a physically constructed rotary double inverted pendulum system to address 12 transition control problems, including swing-up control. We introduced a method for generating feedforward trajectories using the direct collocation technique and

Table 2: Transition times used in the experiments.

Starting EP	Destination EP	T [sec]
EP0	EP1	2.000
	EP2	3.000
	EP3	2.500
EP1	EP0	1.800
	EP2	2.500
	EP3	2.500
EP2	EP0	2.500
	EP1	2.000
	EP3	2.921
EP3	EP0	2.500
	EP1	2.000
	EP2	2.000

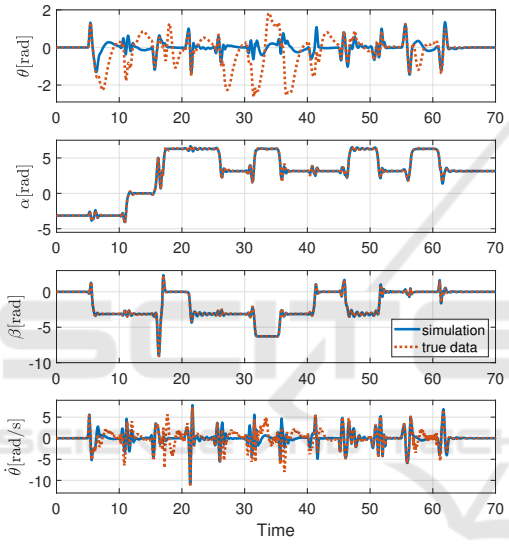

Figure 10: 12-step transition trajectories of the rotary double inverted pendulum: simulated trajectory (solid line) and actual trajectory (dot-dashed line).

implemented these trajectories with a 2-DOF controller incorporating time-varying LQ control. This approach effectively addressed the complex transition control problem by combining feedforward trajectory generation and feedback control. The efficiency and feasibility of the proposed method were demonstrated through continuous control of the 12 transition paths among the four equilibrium points of the double inverted pendulum. The main contributions of this study include the novel definition and experimental implementation of the transition control problem between equilibrium points, extending the existing swing-up problem, and the practical applicability of the proposed control strategy validated through experimental results.

Future research can consider several directions to further develop the transition control method presented in this paper. First, the application of a Disturbance Observer (DOB) technique could enhance the robustness of the system against disturbances. Second, incorporating artificial intelligence-based control techniques such as Reinforcement Learning could lead to the development of more intelligent and adaptive control systems. Third, introducing advanced control strategies, such as nonlinear control techniques or Model Predictive Control (MPC), could be a promising direction to improve the performance of the controller.

As additional research, it is necessary to evaluate the performance of the transition control under various experimental environments and conditions to verify the generality of the proposed method. In the future, this transition control strategy will be applied to multi-dimensional and multi-body systems to explore the controllability of more complex dynamic systems. Through this, it is expected that the method can be developed into a universal control technique applicable not only to the rotary double inverted pendulum system but also to other complex dynamic systems.

ACKNOWLEDGEMENTS

This work was supported by the National Research Foundation of Korea(NRF) grant funded by the Korea government(MSIT)(RS-2024-00347193).

REFERENCES

Baek, J., Lee, C., Lee, Y. S., Jeon, S., and Han, S. (2024). Reinforcement learning to achieve real-time control of triple inverted pendulum. *Engineering Applications of Artificial Intelligence*, 128:107518.

Brown, D. and Strube, M. (2020). Design of a neural controller using reinforcement learning to control a rotational inverted pendulum. In *2020 21st International Conference on Research and Education in Mechatronics (REM)*, pages 1–5.

Åström, K. J. and Furuta, K. (2000). Swinging up a pendulum by energy control. *Automatica*, 36(2):287–295.

Graichen, K., Treuer, M., and Zeitz, M. (2007). Swing-up of the double pendulum on a cart by feedforward and feedback control with experimental validation. *Automatica*, 43:63–71.

Ibrahim, M. M., Ubaid, M. A., Rachid, M., and Maamar, B. (2019). Stabilization of a double inverted rotary pendulum through fractional order integral control scheme. *International Journal of Advanced Robotic Systems*, 16(4).

Ju, D., Choi, C., Jeong, J., and Lee, Y. S. (2022). Design and parameter estimation of a double inverted pendulum for model-based swing-up control. *Journal of In-*

stitute of Control, Robotics and Systems (in Korean), 28(9):793–803.

Kelly, M. (2017). An introduction to trajectory optimization: How to do your own direct collcation. *SIAM Review*, 59(4):849–904.

Liang, F., Xin, X., and Li, Y. (2023). Swing-up and balance control of rotary double inverted pendulum. In *Proceedings of the 2023 3rd International Conference on Robotics and Control Engineering*, page 65–70.

Meta, T., Gyeong, G. Y., Park, J. H., and Lee, Y. S. (2014). Swingup control of an inverted pendulum subject to input/output constraints. *Journal of Institute of Control, Robotics and Systems (in Korean)*, 20:835–841.

Oh, Y. and Lee, Y. S. (2018). Robust Swing-up Control of a Rotary Inverted Pendulum Subject to Input/Output Constraints. *Journal of Institute of Control, Robotics and Systems (in Korean)*, 24(5):423–430.

Rahairi, M., H.Selamat, Zamzuri, H., and Ahmad, F. (2011). Pid controller optimization for a rotational inverted pendulum using genetic algorithm. In *2011 Fourth International Conference on Modeling, Simulation and Applied Optimization*, pages 1–6.

Ratiroch-Anant, P., Anabuki, M., and Hirata, H. (2004). Self-tuning control for rotational inverted pendulum by: eigenvalue approach. In *2004 IEEE Region 10 Conference TENCON 2004.*, volume D, pages 542–545.

Singh, S. and Swarup, A. (2021). Control of rotary double inverted pendulum using sliding mode controller. In *2021 International Conference on Intelligent Technologies (CONIT)*, pages 1–6.

Sondarangallage, D. A. and Manukid, P. (2019). Control of rotary double inverted pendulum system using mixed sensitivity h∞ controller. *International Journal of Advanced Robotic Systems*, 16(2).

Thein, M.-W. and Misawa, E. (1995). Comparison of the sliding observer to several state estimators using a rotational inverted pendulum. In *Proceedings of 1995 34th IEEE Conference on Decision and Control*, volume 4, pages 3385–3390.

Tran, N., Nguyen, V., Le, C., Lai, A., Nguyen, T., Huynh, M., Phan, V., Tong, G., Nguyen, L., and Ngo, T. (2024). Lqr control for experimental double rotary inverted pendulum. *Journal of Fuzzy Systems and Control*, 2(2):104–108.

Zied, B. H., Mohammad, J. F., and Zafer, B. (2020). Development of a Fuzzy-LQR and Fuzzy-LQG stability control for a double link rotary inverted pendulum. *Journal of the Franklin Institute*, 357(15):10529–10556.